ELSEVIER

Magnetic Resonance Materials in Biology, Physics and Medicine 6 (1998) 28–36

MAGMA

Magnetic Resonance Materials in Physics, Biology and Medicine

Diffusion anisotropy measurements in ischaemic stroke of the human brain

P.A. Armitage [a,*], M.E. Bastin [a], I. Marshall [a], J.M. Wardlaw [b], J. Cannon [b]

[a] *Department of Medical Physics, University of Edinburgh, Western General Hospital, Crewe Road, Edinburgh EH4 2XU, UK*
[b] *Department of Clinical Neurosciences, University of Edinburgh, Western General Hospital, Crewe Road, Edinburgh EH4 2XU, UK*

Received 8 December 1997; accepted 20 February 1998

Abstract

Magnetic resonance diffusion imaging was performed on 12 patients presenting with symptoms of acute ischaemic stroke (1–6 days post-ictus). Apparent diffusion coefficient (ADC) and diffusion anisotropy measurements were obtained from ischaemic and contralateral normal regions. ADC measurements were decreased by around 40% in ischaemic regions, indicated by an average stroke to normal ratio of 0.56 ± 0.04 ($p < 0.0001$). The measured anisotropy was shown to be significantly increased in ischaemic regions, using both standard deviation and volume ratio anisotropy indices, which gave stroke to normal ratios of 1.78 ± 0.27 ($p = 0.003$) and 0.87 ± 0.05 ($p = 0.005$) respectively. The effects of gradient interactions, image registration, noise contamination and rotational variance and their implications for the results obtained in this study are discussed.

Keywords: Diffusion-weighted MRI; Apparent diffusion coefficient; Diffusion anisotropy; Acute ischaemic stroke

1. Introduction

Diffusion-weighted MRI (DWI) can be used for early detection of ischaemic regions, as the diffusion coefficient is markedly reduced in these areas [1,2]. The underlying biophysical causes for the reduced diffusion coefficient are not fully understood, although several theories have been proposed [3–7]. For example, it was thought that the reduced apparent diffusion coefficient (ADC) may be due to changes in the permeability of the cell membranes. This is unlikely because Monte Carlo simulations in grey matter have indicated that the ADC is relatively insensitive to changes in the membrane permeability [3]. Another theory is that the alteration in ADC is a result of changes in the restriction of the extracellular diffusion due to the shift of water into the intracellular space and the development of cytotoxic edema. Thus, the cell swelling arising from increased intracellular water causes the path of the extracellular water to become more tortuous, which results in a lower extracellular diffusion coefficient. The increased tortuosity has been supported by tracer experiments and in Monte Carlo simulations, where the change in extracellular diffusion has a significant effect on the ADC value [4]. The reduction in ADC may also be directly related to the development of cytotoxic edema, due to the water shift from extracellular to intracellular space. Indications are that the reduced ADC may be directly related to the intracellular and extracellular space fractions [5]. As the infarct progresses, the ADC begins to return to normal and eventually becomes higher than its pre-stroke normal value when the infarct reaches its chronic state. This behaviour is consistent with disintegrating cell membranes, a decreasing cellular volume fraction and is associated with vasogenic edema [3].

* Corresponding author. Tel.: +44 131 5372511; fax: +44 131 5371026; e-mail: paa@skull.dcn.ed.ac.uk

1352-8661/98/$ - see front matter
PII S1352-8661(98)00007-6

The ADC has been assumed to be an average of the diffusion coefficients in the intracellular and extracellular spaces, resulting from the bi-exponential decay of the signal attenuation against diffusion-weighting b-value, although some recent studies suggest that the decay might be more complicated [8]. In most MR stroke studies so far, monoexponential fits with relatively low b–values have been used (< 1000 s mm^{-2}), which only sample the fast part of the bi-exponential decay, biasing the ADC towards the extracellular diffusion coefficient.

The diffusion theories described above are further complicated by the structure of the tissue in which the infarct occurs. Diffusion in normal white matter is highly anisotropic, whereas diffusion in grey matter is only slightly anisotropic. The high order anisotropy is a result of restricted diffusion caused by white matter fibre bundles, where diffusion occurs preferentially along the fibre direction. Diffusion anisotropy has been demonstrated in normal white matter on many previous occasions [9,10], but studies of changes in anisotropy during stroke have not been extensively reported [11–13]. Maier et al. recently reported results from a study of diffusion anisotropy in eight patients presenting with focal cerebral ischaemia in white and grey matter [11]. They found the anisotropy to be increased in the early acute stage (< 1 day) and then to be decreased during later acute and chronic stages (1–200 days).

In this study, diffusion anisotropy was measured in patients presenting with symptoms of acute ischaemic stroke, to evaluate whether changes occurred and whether these agreed with the known biophysical mechanisms. Factors known to effect diffusion anisotropy measurements such as patient motion, signal to noise ratio (SNR), gradient interactions and rotational variance were investigated to establish their influence on the outcome of anisotropy changes in stroke. The anisotropy differences were described using ipsilateral to contralateral ratios to minimise the effects of rotational variance [14].

2. Theory

The addition of further gradients to conventional NMR experiments alters the echo attenuation and can make the experiment sensitive to diffusional motion, as shown by Stejskal [15]. The resulting echo attenuation shows an exponential dependence which is conveniently described using the attenuation factor b. The ADC can be calculated from diffusion measurements undertaken with two different scalar b-values [16], one of which is usually zero in time limited conventional clinical studies, such that

$$\mathrm{ADC} = \frac{\ln(S_{b_1} - S_{b_2})}{b_2 - b_1}, \tag{1}$$

where S_{b_1}, and S_{b_2} are the signals measured with b-values b_1 and b_2, respectively.

Thus, the ADC can be calculated in a particular direction corresponding to the direction in which the diffusion gradient is applied. This analysis is only suitable for isotropic diffusion when imaging and diffusion gradient interactions are negligible. If the diffusion is anisotropic, or gradient interactions are not negligible, then diffusion should be described by a tensor (**D**) with a corresponding b-matrix [17].

The trace of the diffusion tensor, trace (**D**), provides a rotationally invariant measure of the ADC in a sample. A good approximation can be obtained from three orthogonal diffusion measurements, provided that interactions between diffusion and imaging gradients are negligible.

$$\mathrm{Trace}(\mathbf{D}) = \frac{D_{xx} + D_{yy} + D_{zz}}{3} = \frac{\lambda_1 + \lambda_2 + \lambda_3}{3} \approx \frac{\mathrm{ADC}_x + \mathrm{ADC}_y + \mathrm{ADC}_z}{3} = \mathrm{ADC}_{\mathrm{av}} \tag{2}$$

Above, D_{ii} represent the diagonal elements of the diffusion tensor, λ_{1-3} are the eigenvalues of the diffusion tensor and ADC_i represent ADC measurements obtained in three orthogonal directions. It should be noted that $\mathrm{ADC}_{\mathrm{av}}$ can be used as a good approximation for trace (**D**) only when imaging and diffusion gradient interactions are negligible, or if these interactions have been corrected for.

Anisotropy information can be obtained from the elements of the diffusion tensor. Several scalar indices have been proposed to describe anisotropy effects [2,9,18]. They are generally classified into two types; rotationally variant indices, which depend on the orientation of the measurement axes with respect to the principal diffusion axes and rotationally invariant indices, which are orientation independent. Rotationally variant indices have been derived using the orthogonal gradient method and not the full diffusion tensor analysis. Examples include the standard deviation index A_{SD} [2] and the rotationally variant volume ratio A_{VR} [9] shown in Eqs. (3) and (4), respectively.

$$A_{\mathrm{SD}} = \frac{1}{\sqrt{6}\mathrm{ADC}_{\mathrm{av}}} \sum_{i=x,y,z} \sqrt{(\mathrm{ADC}_i - \mathrm{ADC}_{\mathrm{av}})^2} \tag{3}$$

$$A_{\mathrm{VR}} = \frac{\mathrm{ADC}_x \times \mathrm{ADC}_y \times \mathrm{ADC}_z}{(\mathrm{ADC}_{\mathrm{av}})^3} \tag{4}$$

Where $\mathrm{ADC}_{\mathrm{av}}$ is the average of the three orthogonal ADC measurements. It can be seen that A_{SD} is scaled such that zero represents complete isotropy and one represents highest order anisotropy, whereas A_{VR} is scaled such that zero represents highest order anisotropy and one represents complete isotropy.

The full diffusion tensor equivalent of the standard deviation index given above is of the same form, but with tensor elements substituted for the ADC terms and also an additional term is added which involves the off-diagonal tensor elements. The addition of this term can only increase the value of the anisotropy index and thus the rotationally variant index given above can only underestimate the degree of anisotropy, relative to its tensor equivalent [18]. The rotationally invariant volume ratio is also similar to that given above, but with the eigenvalues of the diffusion tensor substituted in place of the ADC values. Addition of the information contained in the off-diagonal elements of **D** only leads to an increase in the measured diffusion anisotropy [9].

3. Methods

3.1. Acquisition

Diffusion-weighted imaging was implemented on a Siemens 63SP Magnetom clinical scanner, equipped with conventional gradients of maximum amplitude 10 mT m^{-1} and 1 ms rise time. A spin echo based sequence, with an image echo time of TE = 121 ms was adapted with diffusion-sensitising gradient pulses of magnitude $G = 9.64$ mT m^{-1} and duration $\delta = 51$ ms, placed symmetrically around the 180° RF pulse. The separation of the leading edges of the pulses was $\Delta =$ 57.4 ms, leading to a scalar diffusion attenuation b-factor of approximately 700 s mm^{-2}. Motion artefacts were corrected using a non-phase encoded navigator echo (TE = 152 ms). This allowed phase distortions caused by non-rigid body motion to be corrected on a point-by-point basis [19–21]. Artefacts due to pulsatile motion were reduced by cardiac gating of the image acquisition with finger pulse triggering, using a repetition rate of two or three cardiac cycles depending on the patient heart rate.

Diffusion-weighted images were obtained with diffusion gradients applied in three orthogonal directions, corresponding to the left-right (x), anterior-posterior (y) and head-feet (z) directions. A reference image ($b = 0$) was also obtained with the same sequence parameters as above, but with no diffusion gradients applied. Eight transverse slices were obtained for each patient, leading to 32 images in total. All images were obtained with a matrix size of 128 × 128, a slice thickness of 5 mm and a square field of view of 230 mm.

3.2. Post-processing

Raw k-space data was transferred to a Sun Ultrasparc workstation (Sun Microsystems, USA.) for further analysis. Fourier transformation of the navigator data was applied in the frequency encoding direction to yield navigator profiles. Phase angles along these profiles, relative to a reference profile, were then determined using (i) a zero-order phase angle [19], (ii) a zero and first-order phase variation [20] and (iii) independent phase angles for each data point [21]. Image data profiles were then corrected using the navigator phase information and Fourier transformed in the phase-encoding direction. The set of images judged to be the most artefact free were then used for further quantification.

ADC_{av} images were calculated from the navigator corrected image data sets on a pixel-by-pixel basis using Eqs. (1) and (2), to obtain maps of the trace of the diffusion tensor. The ADCs were calculated from the diagonal elements of the b-matrices, used for diffusion tensor imaging, such that remaining gradient interaction effects were negligible and ADC_{av} was found to be a good approximation of trace (**D**). The b-matrices were calculated numerically from the pulse sequence parameters [22]. Rotationally variant anisotropy indices were calculated, again on a pixel-by-pixel basis, using Eqs. (3) and (4), to produce maps of the standard deviation and rotationally variant volume ratio indices. All post-processing was undertaken using 'in house' software written in C. The diffusion-weighted image data sets were aligned using SPM95 (Hammersmith Hospital, London, UK) then ADC_{av} and anisotropy maps recalculated, to investigate the effects of motion on the measured anisotropy. The ADC_{av} and anisotropy maps were then displayed using ANALYZE™ (Biomedical Imaging Resource, Mayo Foundation), where measurements were taken.

3.3. Phantom studies

The algorithms used to calculate ADC_{av} and anisotropy maps for the patient studies were first tested in various phantom experiments, to verify that the algorithms were giving sensible information on the anisotropic behaviour of water in restricted media. ADC_{av} and anisotropy images were calculated for a spherical water phantom, to ensure that the values obtained for the ADC were as expected and that the anisotropy indices indicated that the phantom was isotropic.

Noise is known to contaminate anisotropy images such that the measured anisotropy is increased above its true value, when the level of noise is significant. To evaluate the level of noise contamination in this study, the sequence was tested on isotropic and anisotropic media, at various SNRs and then plots of anisotropy against SNR evaluated. The number of acquisitions were altered to vary the SNR, but no other sequence parameters were changed. The SNR was then measured from the patient images to establish if it was sufficiently large such that noise contamination would have a minimal effect on the measured anisotropy. The SNR

was calculated from the mean signal of the diffusion-weighted images in the region of interest $\bar{S}$ and the standard deviation of the background noise σ_n measured from a region of interest of identical size containing background noise, using the relationship shown in Eq. (5),

$$\mathrm{SNR} = 0.66\frac{\bar{S}}{\sigma_n} \tag{5}$$

where the factor 0.66 accounts for Rayleigh statistics [23].

3.4. Patient Studies

Patients admitted to hospital with a mild stroke within the last 6 days were identified by a stroke physician. Some had a CT scan prior to MR (as CT is the routine examination for stroke in our hospital), while some others went straight to MR. Patients with haemorrhagic lesions were excluded from the study. A set of T_2-weighted whole brain images were obtained first, then the eight slices for DWI were set to cover the area of the brain likely to be involved from the symptoms, whether a relevant lesion was visible on the T_2 images or not.

ADC_{av} and anisotropy images were obtained from 12 patients (mean age 66 ± 4 years). The patients were obtained from a larger study of 36 patients selected using the criteria described above. Of those patients studied, 21 were shown to have hyperintense regions using DWI, and 12 showed images sufficiently free from artefact to enable ADC_{av} and anisotropy images to be calculated. This is in agreement with work previously undertaken, showing the success rate of the navigated diffusion imaging technique [24]. Region of interest (ROI) measurements were obtained from ischaemic and contralateral normal areas of ADC_{av} and anisotropy images, both for the SPM registered and unregistered cases. The ROIs were defined on an average diffusion-weighted image constructed from the three orthogonal diffusion-weighted images and were positioned to include well defined hyperintense regions. Highly dispersed hyperintense regions containing large amounts of normal appearing tissue were excluded from the study.

4. Results

4.1. Phantom studies

The measured ADC_{av} of the spherical water phantom at room temperature was $1.98 \pm 0.09 \times 10^{-3}$ mm^2 s^{-1} and is in good agreement with literature values [25]. The anisotropy indices measured from the spherical water phantom are close to their ideal isotropic values. The standard deviation index was measured as 0.028 ± 0.006 (ideal isotropic case 0) and the volume ratio index was measured as 0.997 ± 0.002 (ideal isotropic case 1). Possible sources of experimental error include noise contamination, thermal convection within the phantom, vibration and hardware instabilities.

Allowing for the possible experimental errors, it would appear that the anisotropy indices do assign isotropic values to a homogeneous medium as would be expected. Fig. 1 shows the effect of noise on the two anisotropy indices, for a water phantom exhibiting isotropic diffusion and an anisotropic vegetable phantom. The figure shows the anisotropy to be increased as the SNR is decreased. This causes isotropic diffusion to be seen as anisotropic, while anisotropic diffusion is overestimated. It is clear from the graphs that the effect of the SNR on the measured anisotropy becomes greater as the SNR decreases.

4.2. Patient studies

An example of a set of diffusion images, obtained from a 38 year old patient presenting with symptoms suggesting a possible left partial anterior circulation infarct (2 days post-ictus), is shown in Fig. 2. The 12 patients showed a mix of white and grey matter infarcts, as classified by a neuroradiologist, with four patients having 'pure' white matter infarcts, seven having mixed white and grey matter and one having a 'pure' grey matter infarct. On average patients underwent DWI 3.4 ± 1.2 days after onset of stroke symptoms. 32 ROI measurements were obtained from the 12 patients, either from the same infarct extending into multiple slices or from a patient having multiple recent infarcts. ROI measurements varied in size from three to 62 pixels (mean 18 ± 3); however no relation was found between the size of the infarct and the measured ADC_{av} or anisotropy. The mean SNR of the patient diffusion-weighted images was found to be 36 ± 3 for normal appearing regions and 72 ± 6 for ischaemic regions, calculated using Eq. (5). The mean ADC_{av}, volume ratio anisotropy and standard deviation anisotropy are shown in Table 1, for the 12 patients. The values are shown for measurements taken from the SPM registered and unregistered images.

One-sample t-tests of the mean stroke to normal ratios for the ADC and anisotropy measurements were performed. The ADC_{av} ratio yielded 0.75 ± 0.07 ($p = 0.0008$) for the unregistered data and 0.56 ± 0.04 ($p < 0.0001$) for the registered data. Similarly, the standard deviation anisotropy test yielded 1.90 ± 0.42 ($p = 0.02$) for the unregistered data and 1.78 ± 0.27 ($p = 0.003$) for the registered data. The volume ratio anisotropy test yielded 0.90 ± 0.08 ($p = 0.12$) for the unregistered data and 0.87 ± 0.05 ($p = 0.005$) for the registered data. ADC and anisotropy stroke to normal ratios were

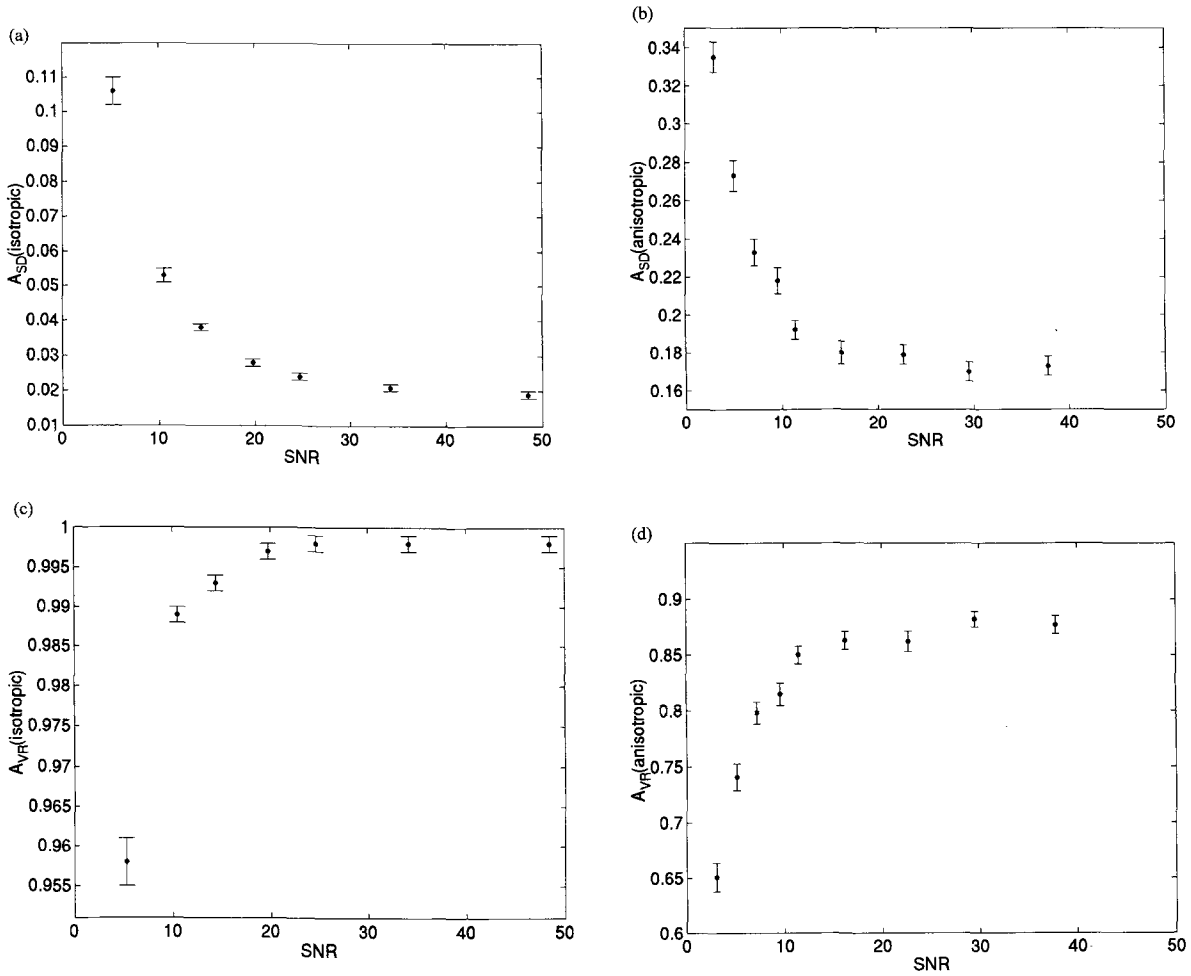

Fig. 1. Variation of diffusion anisotropy indices with signal to noise ratio, for the standard deviation anisotropy index (A_{SD}) in (a) isotropic; and (b) anisotropic; diffusion phantoms and for the volume ratio anisotropy index (A_{VR}) in (c) isotropic; and (d) anisotropic; diffusion phantoms.

found to be identical, to within experimental error, for white and mixed grey matter infarcts, even though white matter regions showed greater levels of anisotropic diffusion.

5. Discussion

The anisotropy measurements were shown to be affected by noise such that the measured anisotropy increased as the SNR decreased as shown in Fig. 1. In this example, the measured anisotropy begins to increase rapidly at SNRs below about 20. At extremely low SNR, the trace of the diffusion tensor also became noticeably elevated. Fig. 1 suggests that the SNR of the brain diffusion images, of around 36 for normal appearing regions and 72 for ischaemic regions, is sufficient such that the effects of noise on the calculated ADC_{av} and anisotropy will be small because the anisotropy is only decreasing by negligible amounts if the SNR is further increased. The average measure of the SNR over the individual ischaemic and normal ROI measurements, rather than the SNR over the whole brain was used because of the CSF present in the brain. CSF has a high diffusion coefficient and thus small signal in the diffusion-weighted images. However, the ROI measurements generally contained relatively small amounts of CSF and so the whole brain estimate of SNR would provide a conservative view of the SNR. The SNR of an ischaemic region was always greater than that of the contralateral normal region and so any small residual noise contamination would be more pronounced in the normal region. This would reduce the anisotropy contrast between stroke and normal regions in the brain and so further supports the observation of increased anisotropy in stroke.

The patient data suggest that registering the original diffusion-weighted images influences the measurements obtained of ADC_{av} and anisotropy, particularly when studying small strokes. The anisotropy appears to be overestimated when the unregistered images are used. This is not entirely surprising as in regions where two different media intersect, a small misregistration could cause the intersection to be seen as a highly anisotropic

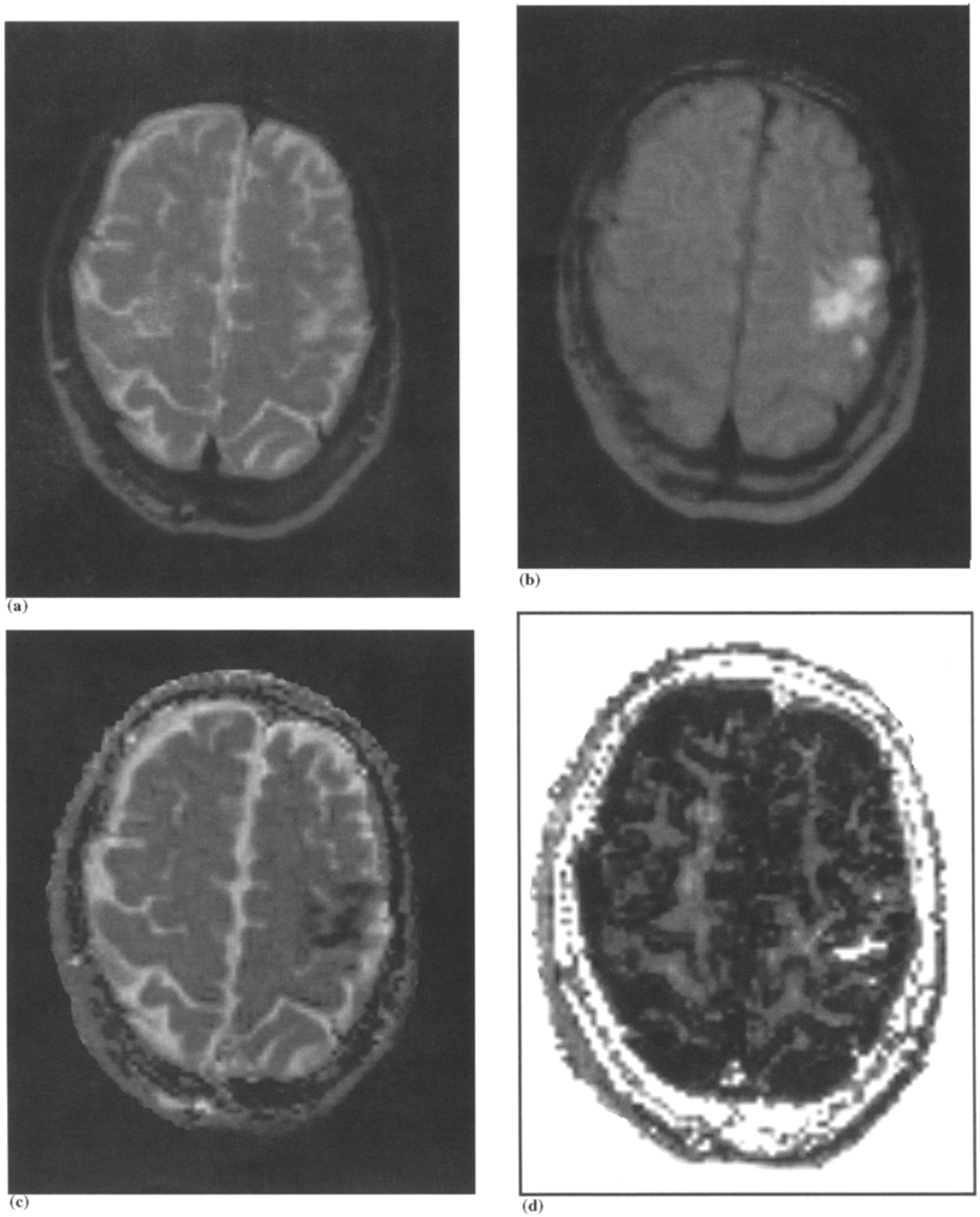

Fig. 2. Examples of (a) T_2-weighted (TE = 121 ms, TR = 2–3 cardiac cycles, FOV = 230 mm); (b) diffusion-weighted (TE = 121 ms, TR = 2–3 cardiac cycles, FOV = 230 mm, $\delta = 51$ ms, $\Delta = 57.4$ ms, $b = 700$ s mm^{-2}); (c) ADC_{av}; (d) standard deviation anisotropy; and (e) volume ratio anisotropy; images for a 38 year old patient presenting with symptoms of a partial anterior circulation infarct (PACI).

region. This would be particularly noticeable in this study where many of the ROIs are small in size. ADC_{av} is also noticeably higher in the unregistered stroke regions, this is probably due to misregistered diffusion-weighted images causing some normal tissue to be included in the ischaemic ROI therefore increasing the measured ADC. Mean translations of 3.2 ± 0.2 mm and mean rotations of $4.6 \pm 0.4°$ were obtained from SPM registration of the 12 patients, suggesting a possible misregistration of one or two pixels between diffu-

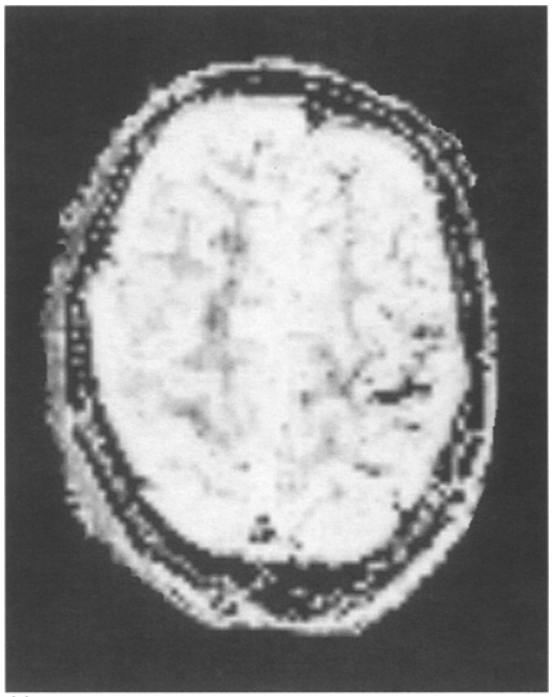

(e)

Fig. 2. (*Continued*)

sion-weighted images. So, while the navigator echo can correct for rotations and translations of this order during the image acquisition, the mean position of the image may be shifted and thus require further alignment when calculating ADC_{av} and anisotropy images.

The ADC measurements obtained from the 12 patients using the registered images suggest an ADC_{av} decrease of about 40% in the ischaemic regions which agrees with previous studies of ADC changes in acute stroke [2,26]. It is clear from the data that the ADC_{av} decrease and anisotropy increase are highly significant ($p \ll 0.05$) when the registered images are used. The changes are much less significant if the calculated images are not obtained from a registered set of diffusion-weighted images. This demonstrates the importance of registering images when calculating ADC and anisotropy maps if quantitative results are to be obtained. This would apply even for rapidly-acquired images (e.g. echo planar imaging) because patient motion between scans may still occur.

Table 1
Average region of interest measurements obtained from stroke and contralateral normal areas of ADC_{av} and diffusion anisotropy maps from 12 patients with small cortical or lacunar infarcts

		Stroke region	Normal region	Stroke/normal ratio
ADC_{av}	Non-registered	0.76 ± 0.06[a]	1.14 ± 0.08[a]	0.75 ± 0.07
	Registered	0.60 ± 0.04[a]	1.15 ± 0.08[a]	0.56 ± 0.04
A_{SD}[b]	Non-registered	0.36 ± 0.04	0.23 ± 0.03	1.90 ± 0.42
	Registered	0.27 ± 0.02	0.18 ± 0.02	1.78 ± 0.27
A_{VR}[b]	Non-registered	0.70 ± 0.04	0.83 ± 0.03	0.90 ± 0.08
	Registered	0.74 ± 0.04	0.86 ± 0.03	0.87 ± 0.05

Results are shown for images calculated from unregistered and registered sets of diffusion-weighted images.
[a] ADC_{av} in 10^{-3} mm^2 s^{-1}.
[b] Notice that A_{SD} is scaled such that 0 represents isotropic diffusion and 1 represents highest order anisotropic diffusion while A_{VR} is scaled such that 1 represents isotropic diffusion and 0 represents highest order anisotropic diffusion.

The increased anisotropy measured in this study seems to support the idea of the cell swelling in cytotoxic edema causing an increased restriction of the extracellular water, which would be accompanied by a reduced ADC and an increase in diffusion anisotropy. The biophysical mechanism for the anisotropy increase is uncertain, but a possible explanation arises if an arrangement of aligned fibre bundles are considered, where diffusion occurs preferentially along the fibre direction. Swelling of the fibres perpendicular to their axis will lead to a reduced space between the fibres. This will increase the restriction of the extracellular water, transverse to the fibre direction, thus increasing the measured anisotropy [11]. Diffusion imaging shows great promise for enabling the extent of this swelling to be observed in vivo by measuring the changes of ADC and diffusion anisotropy. The large variability in ADC and anisotropy between patients can be assigned to the different tissue structures and the degree of cell

swelling, suggesting that classification of infarcts into pure white matter and mixed grey/white matter may be more revealing, for a patient group of sufficient size. However, our preliminary findings suggest that the changes of stroke to normal ratios are the same for both white and grey matter infarcts, so this classification may be unnecessary.

There will also be a degree of rotational variance to the measured anisotropy in this study, which would increase the variability between patients. Together with an underestimation of the anisotropy caused by not sampling the whole diffusion tensor, it would be recommended that the diffusion tensor technique be used for a fully quantitative analysis, particularly in multiple studies. However, in using the three gradient orthogonal technique in a multi-patient study of sufficient size, the stroke to normal ratios should show equal amounts of increased and decreased anisotropy, if there is no underlying difference in anisotropy between the stroke and normal regions. It has previously been demonstrated that using ipsilateral to contralateral ratios provides a method of measuring ADC changes in ischaemia that is independent of tissue orientation [14], although extreme care must be taken when positioning the ROIs if errors are not to be introduced. Similarly, due to the overall symmetry of the brain, anisotropy differences quantified using ipsilateral to contralateral ratios provide a means of measuring these changes that is also largely independent of tissue orientation. So, while the absolute anisotropy may be underestimated using the three gradient orthogonal technique, using the stroke to normal ratios should be sufficient for identifying if the anisotropy is elevated or otherwise in the diseased state, provided that the contralateral side is not diseased. However, this relies on the patients being identically oriented in the scanner to allow comparisons in a multiple study and so the diffusion tensor method is still to be recommended to avoid rotationally variant measures, subject to scan time and hardware considerations.

6. Conclusion

Diffusion imaging has been performed on 12 patients presenting with symptoms of acute ischaemic stroke (1–6 days post-ictus). ADC_{av} measurements show a significant drop of around 40% in acute ischaemic regions. Diffusion anisotropy changes have also been demonstrated and were significantly increased in acute stroke regions. Factors influencing the measured ADC_{av} and anisotropy have been investigated such as signal to noise ratio and image registration. It has been demonstrated that these factors can make a significant difference to the measured anisotropy and their effects have been minimised or accounted for in this study.

Early indications show promise that diffusion anisotropy changes are evident in stroke and could be used to help characterise further ischaemic regions. Preliminary findings suggest that the anisotropy decreases in the later stages of ischaemic stroke due to disintegrating membrane walls, associated with vasogenic edema [11]. Thus, diffusion anisotropy imaging may be useful in characterising acute, sub-acute and chronic strokes. The results obtained in this study show promise that diffusion anisotropy imaging could become a useful method for characterising ischaemic regions, particularly when extended to the fully quantitative diffusion tensor analysis. The technique may also find further possible application in looking at structural disorders such as delayed myelination in neonates [27], characterisation of brain tumors [28], multiple sclerosis and epilepsy.

References

[1] Le Bihan D, Turner R, Douek P, Patronas N. Diffusion MR imaging: clinical applications. AJR 1992;159:591–9.
[2] van Gelderen P, de Vleeschouwer MHM, DesPres D, Pekar J, van Zijl PCM, Moonen CTW. Water diffusion and acute stroke. Magn Reson Med 1994;31:154–63.
[3] Szafer A, Zhong J, Gore JC. Theoretical model for water diffusion in tissues. Magn Reson Med 1995;33:697–712.
[4] Niendorf T, Dijkhuizen RM, Norris DG, van Lookeren Campagne M, Nicolay K. Biexponential diffusion attenuation in various states of brain tissue: implications for diffusion-weighted imaging. Magn Reson Med 1996;36:847–57.
[5] Anderson AW, Zhong J, Petroff OAC, Szafer A, Ransom BR, Pritchard JW, Gore JC. Effects of osmotically driven cell volume changes on diffusion-weighted imaging of the rat optic nerve. Magn Reson Med 1996;35:162–7.
[6] Norris DG, Niendorf T, Hoehn-Berlage M, et al. Incidence of apparent restricted diffusion in three different models of cerebral infarction. Magn Reson Imaging 1994;12:1175–82.
[7] Norris DG, Niendorf T, Leibfritz D. Healthy and infarcted brain tissues studied at short diffusion times: the origins of apparent restriction and the reduction in apparent diffusion coefficient. NMR Biomed 1994;7:304–10.
[8] Assaf Y, Cohen Y. The effect of b value range and diffusion time on the attenuation of brain water signal in diffusion experiments. Proc ESMRMB 14th Annual Meeting, 1997, p. 63.
[9] Pierpaoli C, Basser PJ. Toward a quantitative assessment of diffusion anisotropy. Magn Reson Med 1996;36:893–906.
[10] Moseley ME, Cohen Y, Kucharczyk J, et al. Diffusion-weighted MR imaging of anisotropic water diffusion in cat central nervous system. Radiology 1990;176:439–45.
[11] Maier SE, Gudbjartsson H, Hsu L, Jolesz FA. Diffusion anisotropy imaging of stroke. Proc ISMRM 5th Annual Meeting, 1997, p. 573.
[12] Armitage PA, Marshall I, Wardlaw JM, Cannon J, Diffusion anisotropy in ischaemic stroke. Proc ESMRMB 14th Annual Meeting, 1997, p. 159.
[13] Hoehn-Berlage M, Eis M, Back T, Kohno K, Yamashita K. Changes of relaxation times (T_1, T_2) and apparent diffusion coefficient after permanent middle cerebral artery occlusion in the rat: Temporal evolution, regional extent, and comparison with histology. Magn Reson Med 1995;34:824–34.

[14] Ulug AM, Beauchamp Jr N, Bryan RN, van Zijl PCM. Absolute quantification of diffusion constants in human stroke. Stroke 1997;28:483–90.

[15] Stejskal EO, Tanner JE. Spin diffusion measurements: spin echoes in the presence of a time-dependent field gradient. J Chem Phys 1965;42:288–92.

[16] Le Bihan D, Breton E, Lallemand D, Grenier P, Cabanis E, Laval-Jeantet M. MR imaging of intravoxel incoherent motions: application to diffusion and perfusion in neurologic disorders. Radiology 1986;161:401–7.

[17] Basser PJ, Mattiello J, Le Bihan D. MR diffusion tensor spectroscopy and imaging. Biophys J 1994;66:259–67.

[18] Conturo TE, McKinstry RC, Akbudak E, Robinson BH. Encoding of anisotropic diffusion with tetrahedral gradients: a general mathematical diffusion formalism and experimental results. Magn Reson Med 1996;35:399–412.

[19] Ordidge RJ, Helpern JA, Qing ZX, Knight RA, Nagesh V. Correction of motional artifacts in diffusion-weighted MR images using navigator echoes. Magn Reson Imaging 1994;12:455–60.

[20] Anderson AW, Gore JC. Analysis and correction of motion artifacts in diffusion-weighted imaging. Magn Reson Med 1994;32:379–87.

[21] de Crespigny AJ, Marks MP, Enzmann DR, Moseley ME. Navigated diffusion imaging of normal and ischaemic human brain. Magn Reson Med 1995;33:720–8.

[22] Basser PJ, Mattiello J, Le Bihan D. Estimation of the effective self-diffusion tensor from the NMR spin echo. J Magn Reson B 1994;103:247–54.

[23] Edelstein WA, Bottomley PA, Pfeifer LM. A signal-to-noise calibration procedure for NMR imaging systems. Med Phys 1984;11:180–5.

[24] Marshall I, Wardlaw JM. Comparison of postprocessing techniques for navigated diffusion weighted imaging. Proc ISMRM 5th Annual Meeting, 1997, p. 1725.

[25] Mills R. Self diffusion of normal and heavy water in the range 1–45°. J Phys Chem 1973;77:685–8.

[26] Warach S, Gaa J, Siewert B, Wielopolski P, Edelman RR. Acute human stroke studied by whole brain echo planar diffusion-weighted magnetic resonance imaging. Ann Neurol 1995;37:231–41.

[27] Sakuma H, Nomura Y, Takeda K. Adult and neonatal human brain: diffusional anisotropy and myelination with diffusion-weighted MR imaging. Radiology 1991;180:229–33.

[28] Tsuruda JS, Chew WM, Moseley ME, Norman D. Diffusion-weighted MR imaging of the brain: value of differentiating between extraaxial cysts and epidermoid tumors. AJNR 1990;11:925–31.